Supplementary methods

Mass Spectrometry sample preparation

Cell pellets (1-2 ×106) were lysed in 50 µl of 4% (w/v) SDS, 100 mM DTT, 100 mM Tris.HCl pH 7.5 supplemented with HALT protease and phosphatase inhibitor cocktail (Thermo Scientific). 20 µg of protein was processed into tryptic peptides by the Filter Aided Sample Preparation method[1]. Peptides were desalted and concentrated with Empore-C18 StageTips and eluted with 0.5% (v/v) acetic acid, 80 % (v/v) acetonitrile[2]. Sample volume was reduced by SpeedVac and supplemented with 2 % (w/v) acetonitrile, 0.1% (w/v) Tri-Fluoro-Acetic acid to a final volume of 5 µl. 3 µl of each sample was analysed.

Mass spectrometry data acquisition

Tryptic peptides were separated by nanoscale C18 reverse chromatography coupled on line to an Orbitrap Fusion Tribrid mass spectrometer (Thermo Scientific) via a nanoelectrospray ion source (Nanospray Flex Ion Source, Thermo Scientific). Peptides were loaded on a 20 cm 75–360 µm inner-outer diameter fused silica emitter (New Objective) packed in-house with ReproSil-Pur C18-AQ, 1.9 µm resin (Dr Maisch GmbH). The column was installed on a Dionex Ultimate3000 RSLC nanoSystem (Thermo Scientific) with a MicroTee union formatted for 360-µm outer diameter columns (IDEX) and a liquid junction. The spray voltage was set to 2.15 kV. Buffer A was composed of 0.5 % (w/v) acetic acid and buffer B of 0.5 % (w/v) acetic acid, 80% (w/v) acetonitrile. Peptides were loaded for 17 min at 300 nl/min at 5% (v/v) buffer B, equilibrated for 5 minutes at 5% buffer B (17-22 min) and eluted by increasing (v/v) buffer B from 5-15% (v/v) (22-87 min) and 15-38% (v/v) (87-147 min), followed by a 10-minute wash to 90 % (v/v) buffer B and a 5 min regeneration to 5% (v/v). Survey scans of peptide precursors from 300 to 1600 *m*/*z* were performed at 120K resolution (at 200 *m*/*z*) with a 4E5 × ion count target. Tandem mass spectrometry was performed by isolation with the quadrupole with isolation window 1.6, HCD fragmentation with

normalized collision energy of 30, and rapid scan mass spectrometry analysis in the ion trap. The MS2 ion count target was set to 10E4 and the max injection time was 35 ms. Only those precursors with

charge state 2–7 were sampled for MS2. The dynamic exclusion duration was set to 30 s with a 10 ppm tolerance around the selected precursor and its isotopes. Monoisotopic precursor selection was turned on. The instrument was run in top speed mode with 3 s cycles. All data were acquired with Xcalibur 4.1 software.

RNA sequencing sample preparation, trimming, alignment and differential expression analysis

For the neutrophils from blood, RNA was extracted from TRIzol preparations of granulocytes as per manufacturer's instructions. RNA was used to generate RNA libraries using the Kapa Stranded RNA-seq kit. Paired-end sequencing (100 base-pair (bp)) was performed on Illumina HiSeq 2000 instruments using TruSeq reagents (Illumina, San Diego, CA, USA). Reads from each RNA-seq library were initially subjected to a quality control step, where, based on duplication rates and gene coverage, outliers were identified and discarded from further analysis Paired-end reads of the were trimmed for both PCR and sequencing adapters using Trim Galore!. Trimmed reads were aligned to the Ensembl v70 human transcriptome using Bowtie[3]. MMSEQ 1.0.8a with default parameters was used to quantify gene expression[4,5]. Differential expression was determined using MMDIFF using a two model comparison.

For the $CD34^+$ HSC-derived neutrophils and accompanying healthy blood PMNs, RNA was purified using the QIAamp RNA Blood Mini Kit (Qiagen, Hilden, Germany). cDNA was synthesized with SuperScript™ VILO™ cDNA Synthesis Kit (Thermofisher Scientific, Waltham, Massachusetts, USA) in an Ampliseq plate from the Ion AmpliSeq™ Kit for Chef DL8 (Thermofisher Scientific). The Ion AmpliSeq™ Transcriptome Human Gene Expression Panel, Chef Ready Kit (Thermofisher Scientific) was used to produce amplicons from 50,000 RefSeq genes. Library preparation was done on the Ion Chef sytem (Thermofisher Scientific) and the libraries were sequenced on the Genestudio S5 (Thermofisher Scientific). Differential expression analysis was performed using DESeq2[6], applying a significance threshold of a Benjamini-Hochberg multiple testing corrected p-value of <0.05 and log2 fold change of >1.

Plasma proteomics

Samples were prepared as previously described with the following modifications[7]. Major serum proteins were removed using Top 12 Abundant Protein Depletion Spin columns (Pierce Biotechnology) and the eluate concentrated and buffer exchanged using Amicon Ultra-0.5 Centrifugal Filter Devices (Merck-Millipore). Depleted serum (normalized to 40 µg of protein per sample) was alkylated, reduced and denatured in ammonium bicarbonate (25mM) plus DTT (5mM; GE Healthcare), IAA (50 mM; Sigma Aldrich) and 1% (w/v) sodium deoxycholate. Sequencing-grade trypsin (Promega) was added for an overnight incubation at 37°C. The samples were concentrated using a MiVac vacuum centrifuge GenevacTM (Thermo Fisher Scientific). For data independent acquisition (DIA)/SWATH-MS 100 variable precursor windows optimised for human plasma samples were employed. An Eksigent ekspert nanoLC 400 autosampler and an Eksigent ekspert nanoLC 425 pump (AB Sciex Ltd) coupled to a SCIEX Triple TOF 6600 mass spectrometer with a DuoSpray Ion Source (AB Sciex Ltd) liquid chromatography system was employed. Samples were reconstituted in a buffer containing 5 % (v/v) ACN, 0.1 % (v/v) FA, 100 fmol/µL of PepCalMix (MS Synthetic Peptide Calibration Kit, AB Sciex Ltd) and 10 x iRT (index retention time) standards (Biognosys AG). After reconstitution, 10 µL of sample (containing 8µg of total protein) was injected for chromatographic separation on YMC-Triart C18 column (12nm, 150 x 0.3 mm) coupled to a YMC-Triart C18 pre-column (12nm, 5 x 0.5 mm). Reversed phase chromatography was performed at 30°C with a flow rate of 5 µL/min over a 120-minute gradient. Mobile phase A contained 100 % LC/MS water with 0.1 % (v/v) FA while mobile phase B contained 100 % ACN with 0.1 % (v/v) FA. Samples were run as duplicate injections and blanks were run between each sample. For SWATH-MS analysis samples were eluted with an analytical gradient (3 - 40 % ACN, 0.1 % FA) and a mass spectrometry method with a total duty cycle of 2.8 s comprising a TOF MS1 scan that was acquired over the mass range (m/z) 400 to 1250 followed by 100 SWATH-MS scans (m/z 100-1500) with variable m/z isolation widths, collision energy and collision energy spread. The spray voltage was set at 5500 V. Mass spectrometry-compatible K562 human protein extract (Promega) was reconstituted as detailed for the samples and run as technical control throughout the experiments to ensure chromatography and mass spectrometry were consistent throughout the sample runs. Mass spectrometry data files were searched using openSWATH (Version: 2.0.0). Peptide matches

were scored using pyProphet (version 0.18.3) and the search results aligned using the feature alignment script from MSproteomics tools. Throughout the analysis the random seed was set to 500. Resultant data was transformed and normalized using the Bioconductor (release 3.5) packages SWATH2Stats and MSstats. SWATH-MS runs with a transition level FDR of greater than 0.3 were excluded from the analysis. Missing values were imputed using the Multivariate Imputation by Chained Equations (MICE) package (version 2.3, seed value 500). Mann-Whitney tests were performed to determine statistical significance between conditions.

Cytospin and staining

0.5 x 10^5 cells were cytospun (Shandon CytoSpin II Cytocentrifuge) onto 76 x 26 mm glass microscope slides. The slides were air-dried followed by Giemsa May-Grünwald staining. The slides were incubated for 5 minutes in May-Grünwald, rinsed with deionized water and subsequent stained with Giemsa solution for 30 minutes. After staining, the slides were analysed with Zeiss Scope.A1 microscope.

ROS production

NADPH-oxidase activity was assessed as the release of hydrogen peroxide, determined by the Amplex Red method (Molecular Probes) by neutrophils stimulated with: zymosan (1 mg/ml), serum-treated zymosan (STZ, 1 mg/ml), phorbol-12-myristate-13-acetate (PMA, 100 ng/ml), platelet-activating factor (PAF, 1 μM) followed by formyl-Met-Leu-Phe (fMLF, 1 μM), in the presence of Amplex Red (0.5 μM) and horseradish peroxidase (1 U/ml). Fluorescence was measured at 30-second intervals for 20 minutes with the infinitiPRO2000 plate reader (Tecan, Mannedorf, Switzerland). Maximal slope of H2O2 release was assessed over a 2-minute interval.

Protease activity

Protease release after degranulation was measured by degradation of fluorescent DQ-green BSA (bovine serum albumin) (Life Technologies). Granulocytes at a concentration of 2x106/ml were resuspended in Hepes buffer and incubated with DQ-BSA and 1 μM PAF or 5 ug/ml cytochalasin B for 5 min at 37°C. Then, the cells were stimulated with 1 μM fMLF or 100 ng/ml PMA (all stimuli were purchased from

Sigma-Aldrich, St. Louis, MO, USA). Also, an unstimulated control value and a 100% content value with Triton X-100 (1% w/v) were determined. The the fluorescence was monitored at 120-second intervals for 1 hour by Infinite 200 PRO plate reader (Tecan, Emission 535 nm).

Cell sorting

Neutrophil progenitors from the $CD34^+$ HSC cultures were separated by FACS sorting based on FSC/SSC and the expression of cell surface markers CD15 (FITC-labeled, clone MMA, BD Biosciences), CD11b (APC-labeled, clone D12, BD Biosciences) and CD16 (PE-labeled, clone 3G8, BD Biosciences) on day 10 or day 17 of the cell culture. FACS sorting was performed using BD FACS Aria III (BD biosciences).

Antibodies and flow cytometry

Platelet activation was measured in whole blood assays using flow cytometry. Platelets were left unstimulated or stimulated with increasing doses of ADP (0.075, 0.5 and 1μM). Whole blood was incubated with fibrinogen conjugated to FITC (Agilent Dako Ltd, Ely, UK) and a monoclonal PE-anti P-selectin antibody (Bristol Institute for Transfusion Science). Platelet activation was measured using a Beckman Coulter FC500 flow cytometer. Percent positive activation of unstimulated platelet were calculated using thresholds generated with a PE isotype control (Bristol Institute for Transfusion Science) or a negative EDTA fibrinogen binding control. Bank of Controls included 57 healthy individuals recruited for platelet function studies by the NIHR-BioResource, were used as a second control group.

The following directly conjugated antibodies were used for cell surface expression of neutrophils derived from blood of healthy donors and GPS patients: PE-labeled anti-CD62L (L-selectin, BD Biosciences), FITC-labeled anti-CD16 (BD Biosciences) and FITC-labeled anti-CD64 (Bio-Rad Laboratories). Flow cytometry data were acquired using Canto II flow cytometer (BD Biosciences) and analyzed using FlowJo software (Tree Star, USA).

Reference List

1. Wisniewski JR, Zougman A, Nagaraj N, Mann M. Universal sample preparation method for proteome analysis. *Nat Methods*. 2009;6(5):359-362.
2. Rappsilber J, Ishihama Y, Mann M. Stop and go extraction tips for matrix-assisted laser desorption/ionization, nanoelectrospray, and LC/MS sample pretreatment in proteomics. *Anal Chem*. 2003;75(3):663-670.
3. Langmead B, Trapnell C, Pop M, Salzberg SL. Ultrafast and memory-efficient alignment of short DNA sequences to the human genome. *Genome Biol*. 2009;10(3):R25.
4. Turro E, Astle WJ, Tavare S. Flexible analysis of RNA-seq data using mixed effects models. *Bioinformatics*. 2014;30(2):180-188.
5. Turro E, Su SY, Goncalves A, Coin LJ, Richardson S, Lewin A. Haplotype and isoform specific expression estimation using multi-mapping RNA-seq reads. *Genome Biol*. 2011;12(2):R13.
6. Love MI, Huber W, Anders S. Moderated estimation of fold change and dispersion for RNA-seq data with DESeq2. *Genome Biol*. 2014;15(12):550.
7. Proc JL, Kuzyk MA, Hardie DB, et al. A quantitative study of the effects of chaotropic agents, surfactants, and solvents on the digestion efficiency of human plasma proteins by trypsin. *J Proteome Res*. 2010;9(10):5422-5437.

Supplementary Figure and Table Legends

Supplementary Figure 1. Neutrophils of GPS patients differ from neutrophils of healthy control in granularity and nucleid acid content. Flow cytometric analysis of GPS patients compared to approximately 500 control individuals indicate that patient neutrophils are less granular (Neut X) and have less nucleic acid content (Neut Y). Neutrophil parameters measured using a Sysmex XN Hematology Analyser (see also Sims *et al*. 2020, ref 26).

Supplemental Figure 2. P-selectin exposure is increased on resting platelets of GPS patients compared to control individuals. A-B) Expression of P-selectin on resting platelets from GPS patients (n=4), day controls (n=4) and from our bank of healthy controls (n=57). **C)** Bound fibrinogen in resting platelets from GPS patients (n=4), day controls (n=4) and from our bank of healthy controls (n=57) measured by flow cytometry. **D-E)** P-selectin expression (D) and fibrinogen binding (E) of platelets from GPS patients (indicated in red, n=3) and day controls (indicated in black, n=3) were measured by flow cytometry after stimulation with increased doses of ADP: 0.075 μM (low), 0.05 μM (medium) and 1 μM (high). Unpaired 2-tailed t test was used. **, $p < 0.01$, ***, $p < 0.001$, ****, $p<0.0001$.

Supplemental Figure 3. Mapping of NBEAL2 peptides identified by mass spectrometry. Alignment of mass spectrometry identified peptides with the canonical NBEAL2 sequence (Uniprot identifier Q6ZNJ1) and NBEAL2 isoforms (shown in blue). Grey tracks represent individual samples or Uniprot sequences. Light blue indicates peptides that were identified by MS/MS. Red represent peptides that were identified by the 'match-between-runs' feature of the MaxQuant software package. Amino acid sequences of peptides that were identified in more than two GPS patients are specified. Patient 1, 7 and 8 are patient C, L and M from table 1, respectively.

Supplemental Figure 4. Characterization of MPB CD34$^+$ HSC-derived neutrophils. A) Representative cytospin of MPB CD34$^+$ HSC-derived neutrophils at the end of differentiation after May-Giemsa staining (objective 40x). **B**) NADPH-oxidase activity of neutrophils from blood (PMN, black

bars) and CD34^{+} HSC-derived neutrophils (grey bars). n=4 **C)** Protease activity of neutrophils from blood (PMN, black bars) and CD34^{+} HSC-derived neutrophils (grey bars). n=5. **D-F)** Killing of *S. aureus* (D), *E. coli* (E) and *C. albicans* (F) was assessed with neutrophils from healthy controls or MPB CD34^{+} HSC-derived neutrophils. The microbial viability was quantified as colony-forming units (CFU) and expressed as a percentage relative to the CFU at the start of the assay. **G-H)** Immuno-EM identification of (G) MPO-positive azurophilic granules (left image 2 µm scale bar, right zoom-in image 500 nm scale bar) and (H) lactoferrin-positive specific granules (left image 1 µm scale bar, right zoom-in image 500 nm scale bar) in MPB CD34^{+} HSC-derived neutrophils. **I-J)** MPB CD34^{+} HSC-derived neutrophils (grey bars) were stimulated with cytochalasin-B (5 µg/ml)/fMLF (1 µM) or PAF (1 µM)/fMLF (1 µM), and the plasma membrane expression of CD66b (specific granule marker) (I) and CD63 (azurophilic granule marker) (J) were measured by flow cytometry. Results are means ± SEM, n=3-5. Unpaired 2-tailed *t* test was used. *, $p < 0.05$, **, $p < 0.01$, ***, $p < 0.001$, ****, $p < 0.0001$.

Supplementary Figure 5. MPB CD34^{+} HSC-derived neutrophils versus bone marrow derived neutrophil progenitors. A) Examples of flow cytometric analysis of sorted PMN progenitor stages from bone marrow (top panel, left plot) and blood derived PMNs (top panel, right plot) from Hoogendijk *et. al.* and MPB CD34^{+} HSCs *in vitro* differentiation towards PMNs (at end of differentiation) based on CD16 and CD11b antibody staining (lower plot). **B**) Line plots representing Pearson correlation coefficients between proteomes of CD16^{NEG}, CD16^{DIM} and CD16^{POS} cultured MPB CD34^{+} HSCs versus *in vivo* obtained bone marrow PMN progenitors and blood derived PMNs. Pink bars indicate highest Pearson correlation coefficients per panel. PM: (pro)myelocytes; MM: metamyelocytes; BN: immature neutrophils with a band-formed nucleus; SN: mature neutrophils with segmented nuclei; PMN: circulating neutrophils derived from blood.

Supplementary Figure 6. NBEAL2 abundancy increases with maturation of MPB CD34^{+} HSC-derived neutrophils and correlates with SG/GG granule protein levels. A) PCA analysis of proteomes of blood circulating neutrophils and MPB CD34^{+} HSCs *in vitro* differentiation towards PMNs. **B)** Heatmap of statistically significantly abundant proteins compared between blood circulating

neutrophils and MPB CD34^{+} HSCs *in vitro* differentiation towards PMNs. **C)** Profile plot of NBEAL2 label-free intensity values. **D)** Stacked bar plots showing proportions of measured granule protein content between MPB CD34^{+} HSC cultured CD16^{POS} versus blood derived PMNs. **E)** Profile plot of z-scored label-free intensity values of SG/GG-annotated proteins. **F)** Boxplot of Pearson correlation coefficient of SG/GG protein correlation with NBEAL2 expression.

Supplementary Figure 7. NBEAL2 transcript levels increase with maturation of MPB CD34^{+} HSC-derived neutrophils but does not correlate with SG/GG granule RNA levels. A) PCA analysis of transcript levels of blood circulating neutrophils and MPB CD34^{+} HSCs *in vitro* differentiation towards PMNs. **B)** Heatmap of statistically significantly abundant transcriptomes compared between blood circulating neutrophils and MPB CD34^{+} HSCs *in vitro* differentiation towards PMNs. **C)** Dotplot of NBEAL2 relative expression levels (rlog). **D)** Violin plot of z-scored relative expression levels of SG annotated proteins.

Supplementary Figure 8. Yield of the CD34^{+} HSCs *in vitro* differentiation towards PMNs. The amount of cells was measured during the CD34^{+} HSC cultures from either PBMCs from healthy donors or GPS patients or from G-CSF mobilized peripheral blood (MPB) of healthy stem cell donors. The cell count was normalized for the starting input of cells on day 0. Results are means ± SEM, n=4-8.

Supplementary Figure 9. Transcript analysis between control and GPS CD34^{+} HSC *in vitro* differentiation towards PMNs revealed no distinct differences. PCA analysis of transcript levels of the sorted neutrophil cell populations (based on maturation markers CD11b and CD16) at the end of differentiation (Day 17) between control and GPS CD34^{+} HSC in vitro differentiation towards PMNs (n=2) or between blood circulating neutrophils from GPS patients or healthy controls (n=2). p = positive, m = min/negative.

Supplementary Figure 10. Normal ROS production by the NADPH oxidase system and protease activity in GPS neutrophils. A) NADPH-oxidase activity of neutrophils from healthy control (black

bars) and from GPS patients (grey bars). Maximal slope of H2O2 release was assessed over a 2-minute interval, n=5. **B)** Protease activity of neutrophils from healthy control (black bars) and from GPS patients (grey bars), n=6. Results are means ± SEM, unpaired 2-tailed *t*-test was used. *, $p < 0.05$.

Supplemental Figure 11. Live cell imaging of PMA induced NETosis. Neutrophils of healthy donors (left) or GPS patients (right) were stained with Quant-iT PicoGreen®dsDNA kit (in red), stimulated with PMA and imaged for 4 hours. Shown are representative images of Supplemental Movie 1 (left) and Supplemental Movie 2 (right) after approximately 3.5 hours. Both the control and GPS neutrophils show chromatin swelling and cell rounding (white arrows), but the cell membrane of the majority of the GPS neutrophils do not rupture in the final stage of NET release. Black arrows indicate rupture of cell membrane.

Supplemental Figure 12. Neutrophils of GPS patients show normal expression of L-selectin, CD16 and CD64. Flow cytometric analysis of L-selectin (CD62L), CD16 and CD64 surface expression of neutrophils from GPS patients (grey bars, n=5-9) and control individuals (black bars, n=8). Results are means ± SEM.

Supplementary Table 1. Differently abundant proteins between GPS patient and healthy control neutrophils. Results of the comparison between GPS and control neutrophils, without the restriction of a two-fold increase or decrease in abundance as shown in Table 2. Proteins in bold indicate the proteins highlighted in the volcano plot of Figure 2A. * possible contamination.

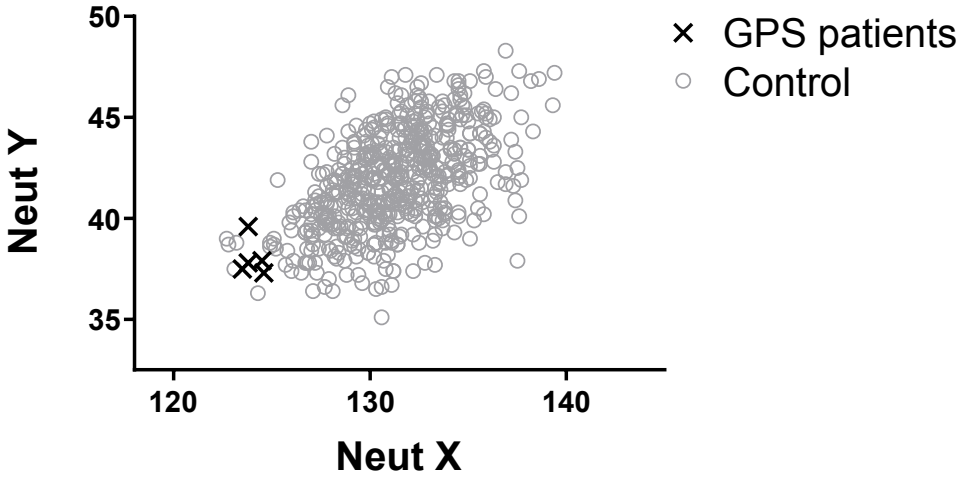

Supplementary Figure 1. Neutrophils of GPS patients differ from neutrophils of healthy control in granularity and nucleid acid content. Flow cytometric analysis of GPS patients compared to approximately 500 control individuals indicate that patient neutrophils are less granular (Neut X) and have less nucleic acid content (Neut Y). Neutrophil parameters measured using a Sysmex XN Hematology Analyser (see also Sims *et al.* 2020, ref 26).

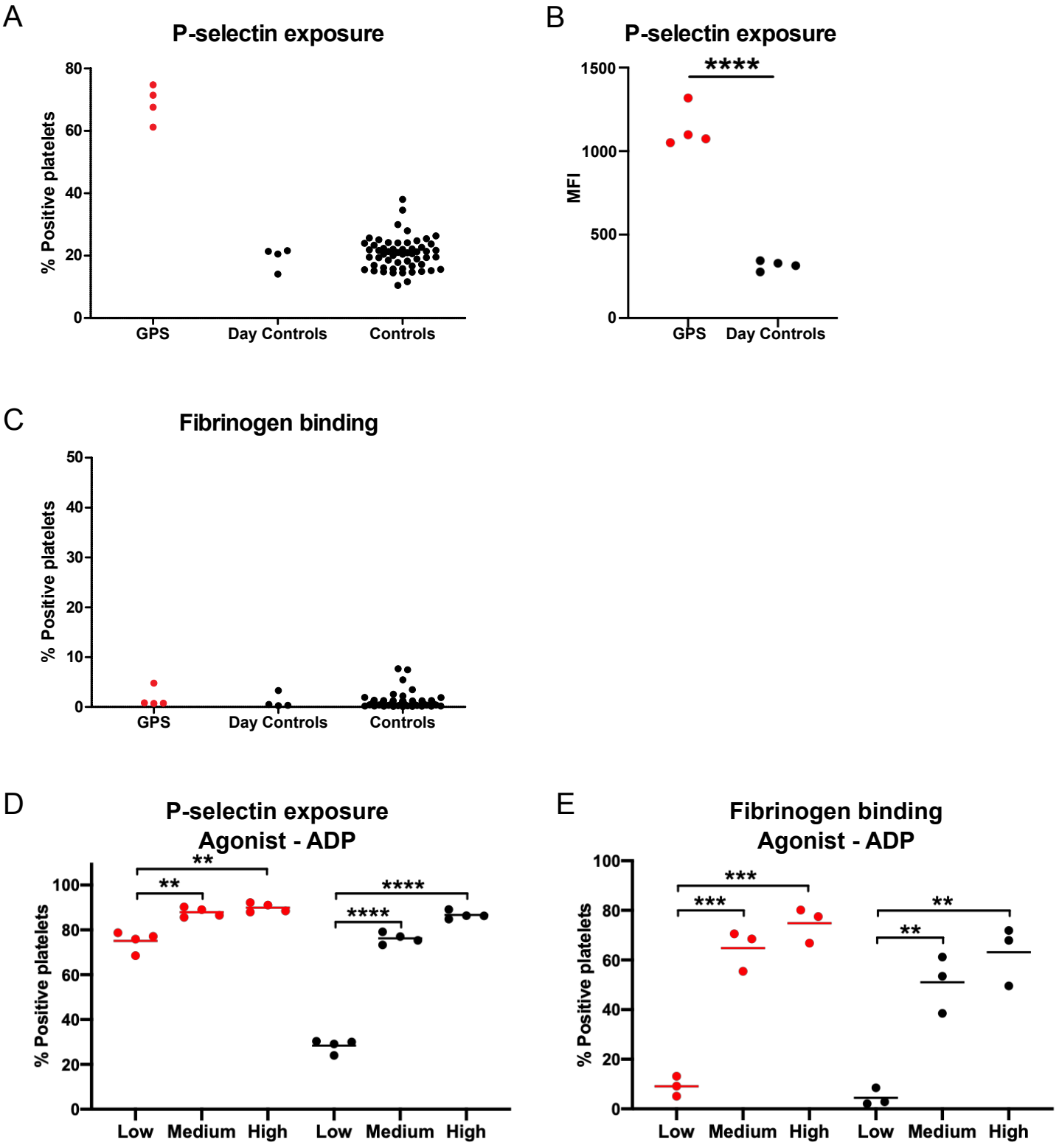

Supplemental Figure 2. P-selectin exposure is increased on resting platelets of GPS patients compared to control individuals. A-B) Expression of P-selectin on resting platelets from GPS patients (n=4), day controls (n=4) and from our bank of healthy controls (n=57). **C)** Bound fibrinogen in resting platelets from GPS patients (n=4), day controls (n=4) and from our bank of healthy controls (n=57) measured by flow cytometry. **D-E)** P-selectin expression (D) and fibrinogen binding (E) of platelets from GPS patients (indicated in red, n=3) and day controls (indicated in black, n=3) were measured by flow cytometry after stimulation with increased doses of ADP: 0.075 µM (low), 0.5 µM (medium) and 1 µM (high). Unpaired 2-tailed t test was used. **, p<0,01, ***, p<0,001, ****, p<0.0001.

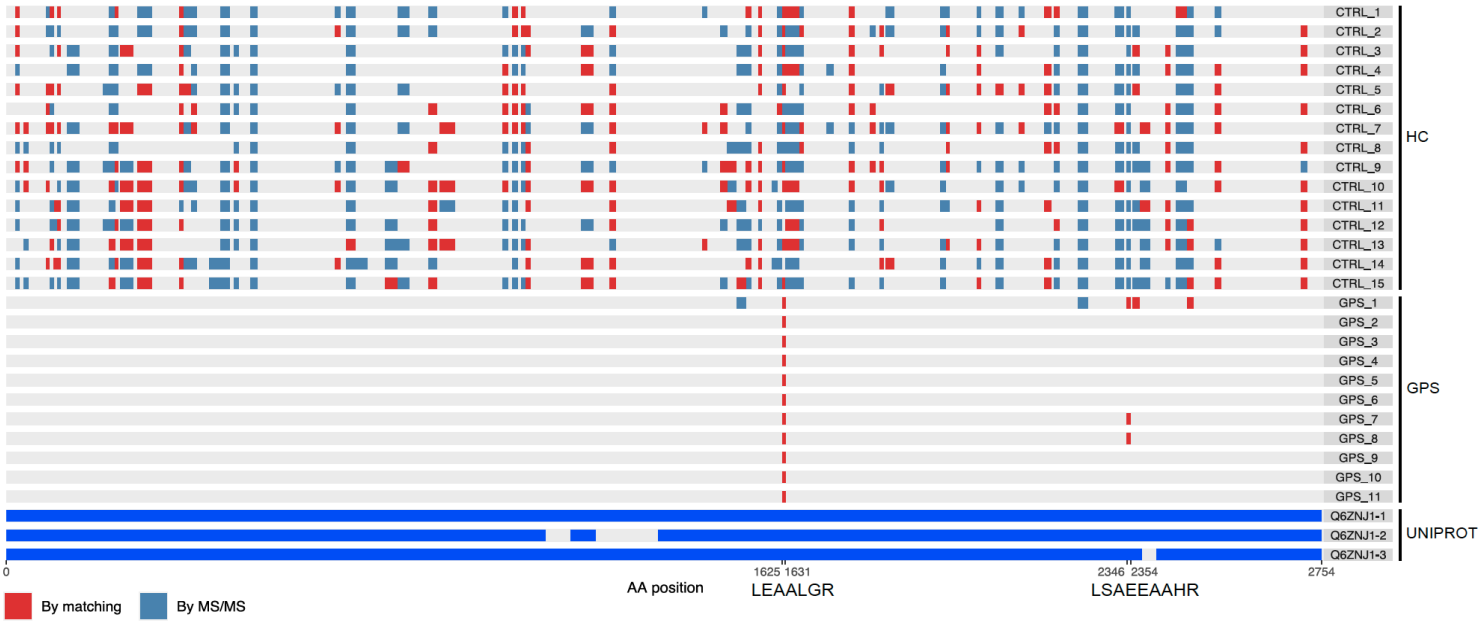

Supplemental Figure 3. Mapping of NBEAL2 peptides identified by mass spectrometry. Alignment of mass spectrometry identified peptides with the canonical NBEAL2 sequence (Uniprot identifier Q6ZNJ1) and NBEAL2 isoforms (shown in blue). Grey tracks represent individual samples or Uniprot sequences. Light blue indicates peptides that were identified by MS/MS. Red represent peptides that were identified by the 'match-between-runs' feature of the MaxQuant software package. Amino acid sequences of peptides that were identified in more than two GPS patients are specified. Patient 1, 7 and 8 are patient C, L and M from table 1, respectively.

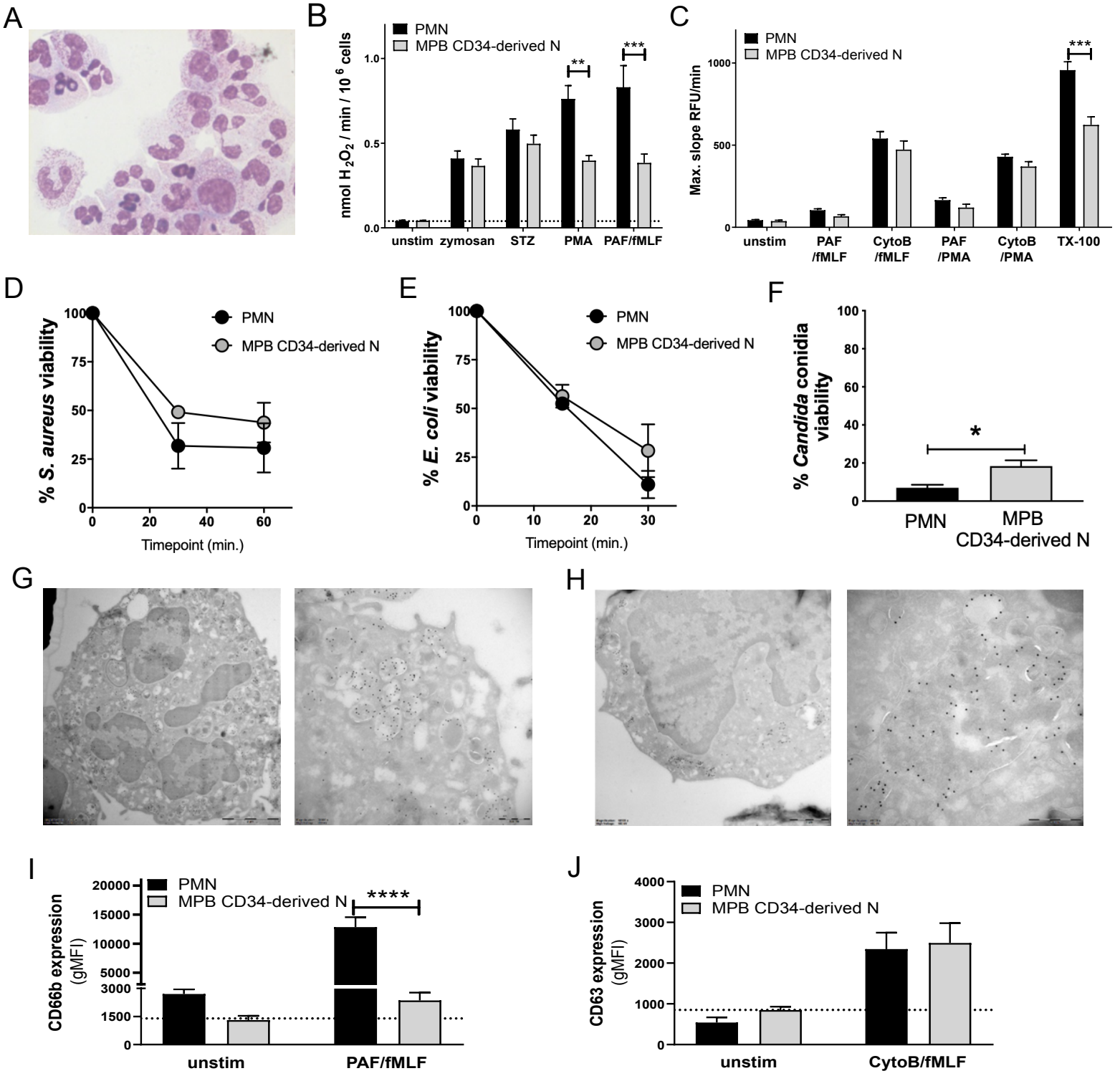

Supplemental Figure 4. Characterization of MPB CD34$^+$ HSC-derived neutrophils. A) Representative cytospin of MPB CD34$^+$ HSC-derived neutrophils at the end of differentiation after May-Giemsa staining (objective 40x). **B)** NADPH-oxidase activity of neutrophils from blood (PMN, black bars) and CD34$^+$ HSC-derived neutrophils (grey bars), n=4. **C)** Protease activity of neutrophils from blood (PMN, black bars) and CD34$^+$ HSC-derived neutrophils (grey bars), n=5. **D-F)** Killing of S. aureus (D), E. coli (E) and C. albicans (F) was assessed with neutrophils from healthy controls or MPB CD34$^+$ HSC-derived neutrophils. The microbial viability was quantified as colony-forming units (CFU) and expressed as a percentage relative to the CFU at the start of the assay. **G-H)** Immuno-EM identification of (G) MPO-positive azurophilic granules (left image 2 µm scale bar, right zoom-in image 500 nm scale bar) and (H) lactoferrin-positive specific granules (left image 1 µm scale bar, right zoom-in image 500 nm scale bar) in MPB CD34$^+$ HSC-derived neutrophils. **I-J)** MPB CD34$^+$ HSC-derived neutrophils (grey bars) were stimulated with cytochalasin-B (5 µg/ml)/fMLF (1 µM) or PAF (1 µM)/fMLF (1 µM), and the plasma membrane expression of CD66b (specific granule marker) (I) and CD63 (azurophilic granule marker) (J) were measured by flow cytometry. Results are means ± SEM, n=3-5. Unpaired 2-tailed t test was used. *, $p < 0.05$, **, $p < 0.01$, ***, $p < 0.001$, ****, $p < 0.0001$.

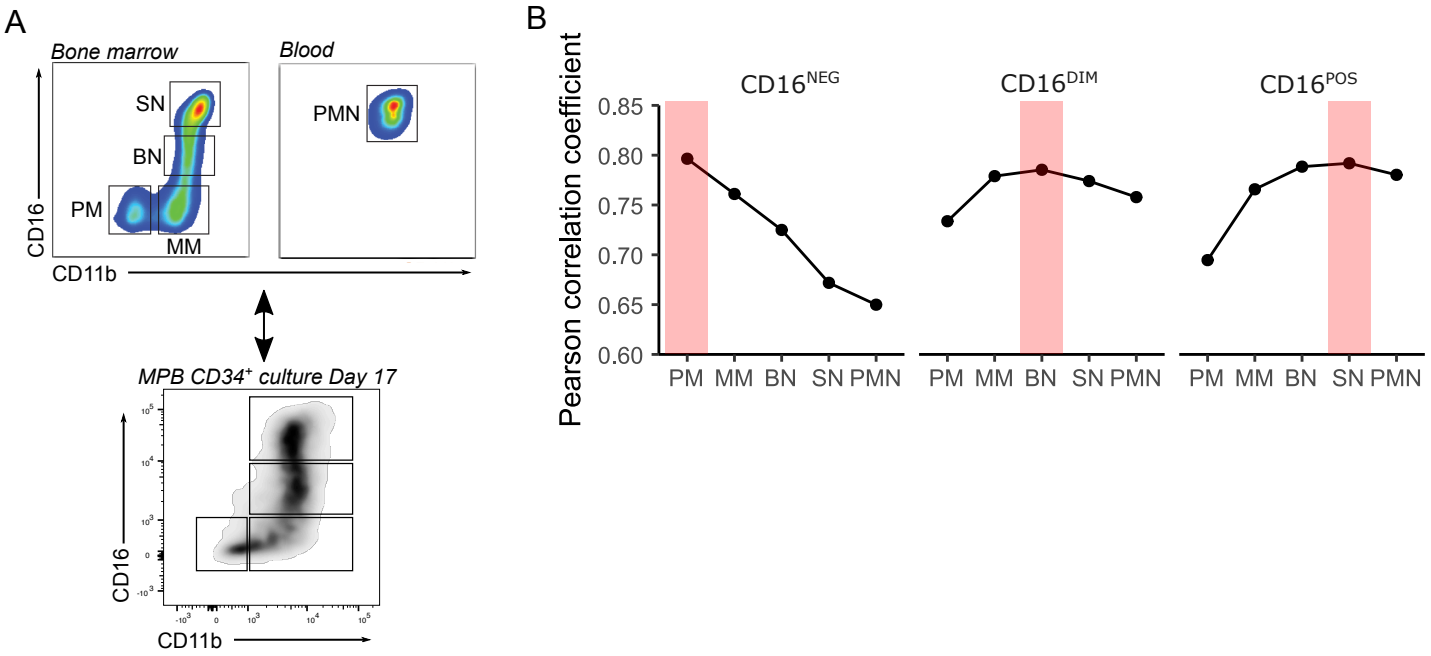

Supplementary Figure 5. MPB CD34^{+} HSC-derived neutrophils versus bone marrow derived neutrophil progenitors. A) Examples of flow cytometric analysis of sorted PMN progenitor stages from bone marrow (top panel, left plot) and blood derived PMNs (top panel, right plot) from Hoogendijk et. al. and MPB CD34+ HSCs in vitro differentiation towards PMNs (at end of differentiation) based on CD16 and CD11b antibody staining (lower plot). **B)** Line plots representing Pearson correlation coefficients between proteomes of CD16^{NEG}, CD16^{DIM} and CD16^{POS} cultured MPB CD34^{+} HSCs versus in vivo obtained bone marrow PMN progenitors and blood derived PMNs. Pink bars indicate highest Pearson correlation coefficients per panel. PM: (pro)myelocytes; MM: metamyelocytes; BN: immature neutrophils with a band-formed nucleus; SN: mature neutrophils with segmented nuclei; PMN: circulating neutrophils derived from blood.

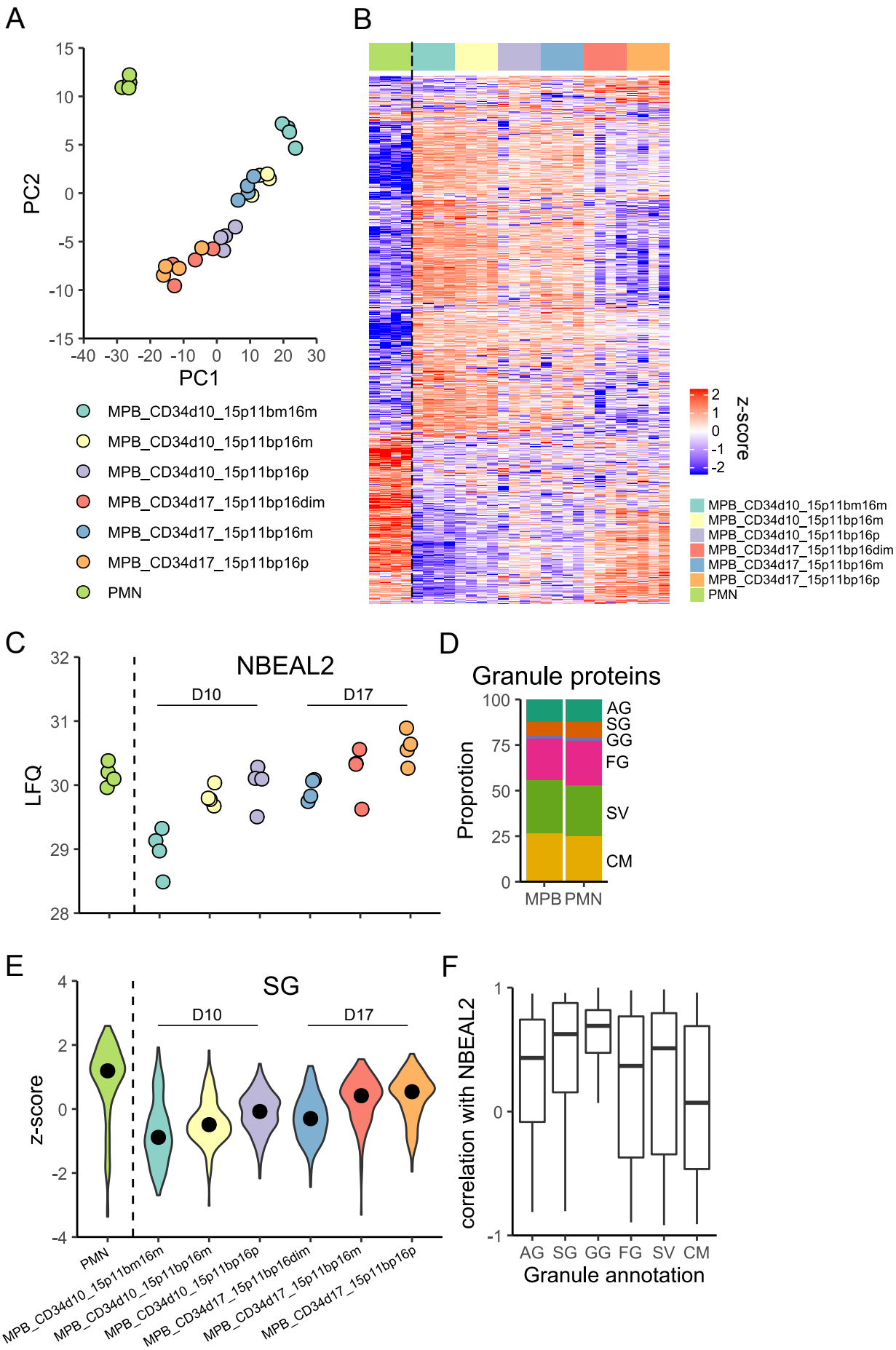

Supplementary Figure 6. NBEAL2 abundancy increases with maturation of MPB CD34^{+} HSC-derived neutrophils and correlates with SG/GG granule protein levels. A) PCA analysis of proteomes of blood circulating neutrophils and MPB CD34^{+} HSCs in vitro differentiation towards PMNs. **B)** Heatmap of statistically significantly abundant proteins compared between blood circulating neutrophils and MPB CD34^{+} HSCs in vitro differentiation towards PMNs. **C)** Profile plot of NBEAL2 label-free intensity values. **D)** Stacked bar plots showing proportions of measured granule protein content between MPB CD34^{+} HSC cultured CD16^{POS} versus blood derived PMNs. **E)** Profile plot of z-scored label-free intensity values of SG/GG-annotated proteins. **F)** Boxplot of Pearson correlation coefficient of SG/GG protein correlation with NBEAL2 expression.

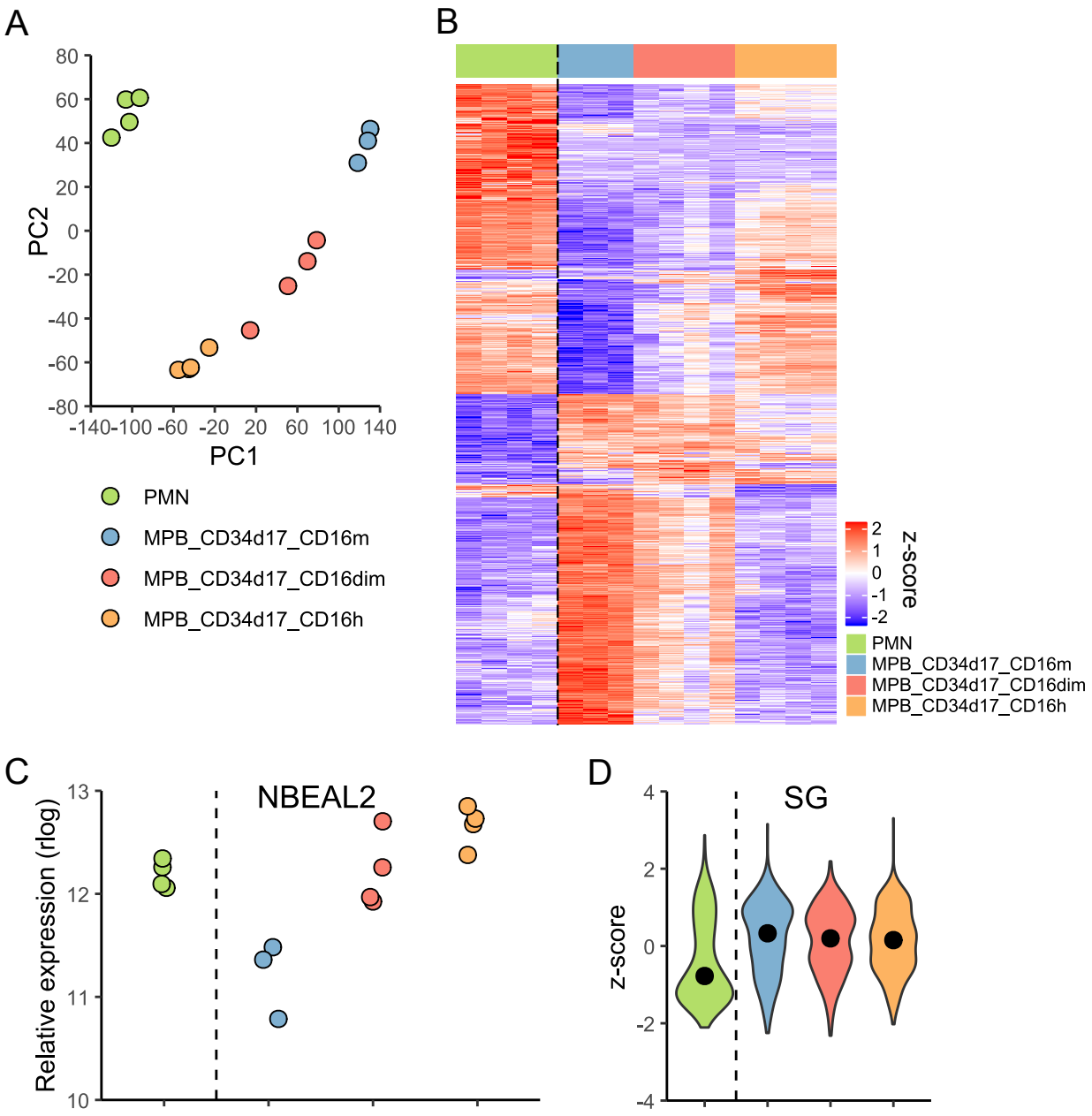

Supplementary Figure 7. NBEAL2 transcript levels increase with maturation of MPB CD34$^+$ HSC-derived neutrophils but does not correlate with SG/GG granule RNA levels. A) PCA analysis of transcript levels of blood circulating neutrophils and MPB CD34$^+$ HSCs *in vitro* differentiation towards PMNs. **B)** Heatmap of statistically significantly abundant transcriptomes compared between blood circulating neutrophils and MPB CD34$^+$ HSCs *in vitro* differentiation towards PMNs. **C)** Dotplot of NBEAL2 relative expression levels (rlog). **D)** Violin plot of z-scored relative expression levels of SG annotated proteins.

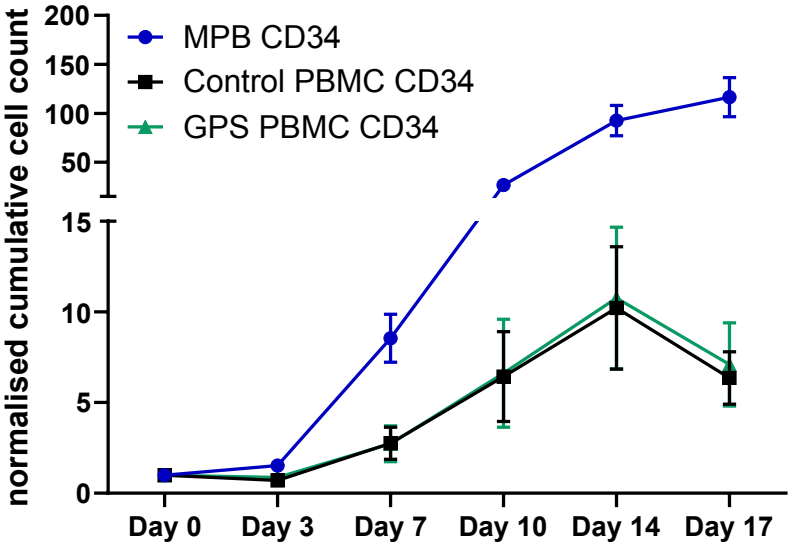

Supplementary Figure 8. Yield of the CD34+ HSCs *in vitro* differentiation towards PMNs. The amount of cells was measured during the $CD34^+$ HSC cultures from either PBMCs from healthy donors or GPS patients or from G-CSF mobilized peripheral blood (MPB) of healthy stem cell donors. The cell count was normalized for the starting input of cells on day 0. Results are means ± SEM, n=4-8.

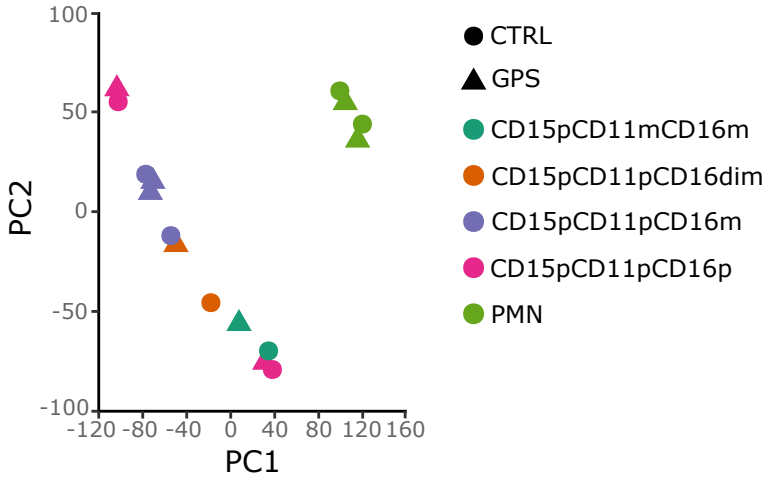

Supplementary Figure 9. Transcript analysis between control and GPS CD34^{+} HSC *in vitro* differentiation towards PMNs revealed no distinct differences. PCA analysis of transcript levels of the sorted neutrophil cell populations (based on maturation markers CD11b and CD16) at the end of differentiation (Day 17) between control and GPS CD34^{+} HSC in vitro differentiation towards PMNs (n=2) or between blood circulating neutrophils from GPS patients or healthy controls (n=2). p = positive, m = min/negative.

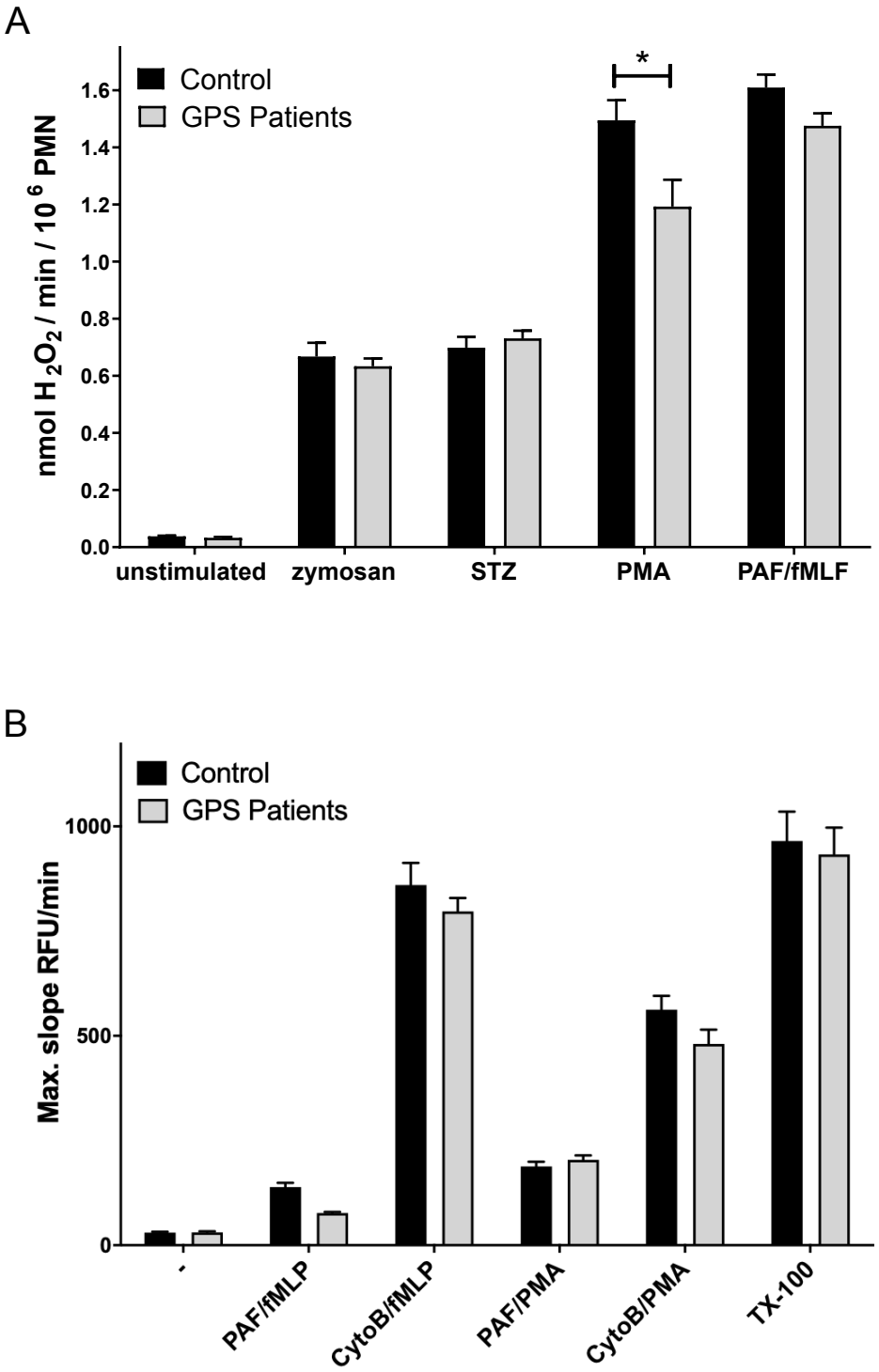

Supplementary Figure 10. Normal ROS production by the NADPH oxidase system and protease activity in GPS neutrophils. A) NADPH-oxidase activity of neutrophils from healthy control (black bars) and from GPS patients (grey bars). Maximal slope of H_2O_2 release was assessed over a 2-minute interval, n=5. **B)** Protease activity of neutrophils from healthy control (black bars) and from GPS patients (grey bars), n=6. Results are means ± SEM, unpaired 2-tailed t-test was used. *, $p < 0.05$.

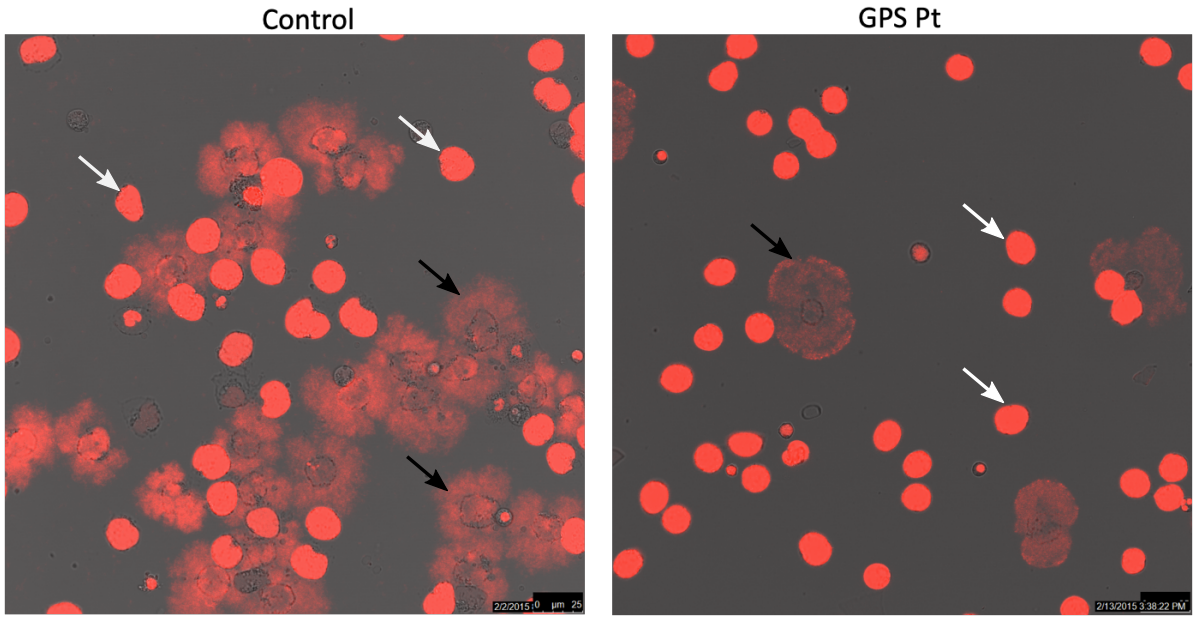

Supplemental Figure 11. Live cell imaging of PMA induced NETosis. Neutrophils of healthy donors (left) or GPS patients (right) were stained with Quant-iT PicoGreen® dsDNA kit (in red), stimulated with PMA and imaged for 4 hours. Shown are representative images of Supplemental Movie 1 (left) and Supplemental Movie 2 (right) after approximately 3,5 hours. Both the control and GPS neutrophils show chromatin swelling and cell rounding (white arrows), but the cell membrane of the majority of the GPS neutrophils do not rupture in the final stage of NET release. Black arrows indicate rupture of cell membrane.

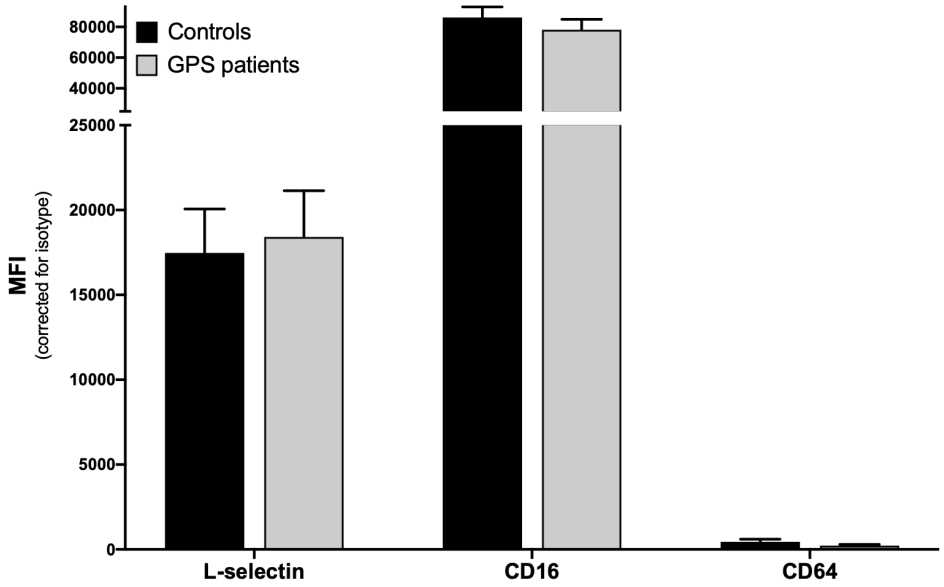

Supplemental Figure 12. Neutrophils of GPS patients show normal expression of L-selectin, CD16 and CD64. Flow cytometric analysis of L-selectin (CD62L), CD16 and CD64 surface expression of neutrophils from GPS patients (grey bars, n=5-9) and control individuals (black bars, n=8). Results are means ± SEM.